



Transfer of environmental signals from surface to the underground at Ascunsă Cave, Romania

Virgil Drăgușin¹, Sorin Balan², Dominique Blamart³, Ferenc L. Forray⁴, Constantin Marin¹, Ionuț Mirea^{1,4}, Viorica Nagavciuc⁵, Aurel Perșoiu^{5,6}, Laura Tîrlă⁷, Alin Tudorache¹, Marius Vlaicu¹

¹Emil Racoviță Institute of Speleology, Frumoasă St. 31, 010986, Romania

²National Research and Development Institute for Marine Geology and Geoecology, Mamaia Blvd. 304, Constanța, 900581, Romania

³Laboratoire des Sciences du Climat et de l'Environnement LSCE-IPSL CEA-CNRS-UVSQ, Paris-Saclay, Avenue de la Terrasse, Bât. 12 91198 Gif-Sur-Yvette CEDEX – France

⁴Department of Geology, Babeș -Bolyai University, Kogălniceanu 1, 400084 Cluj-Napoca, Romania

⁵Stable Isotope Laboratory, Ștefan cel Mare University, Universității 13, Suceava 720229, Romania

⁶Emil Racoviță Institute of Speleology, Clinicilor 5, Cluj Napoca 400006, Romania

⁷Department of Geography, University of Bucharest, N. Bălcescu Street 1, Romania

Correspondence to: Virgil Drăgușin (virgil.dragusin@iser.ro)

Abstract. We present here the results of a four year environmental monitoring program at Ascunsă Cave, Romania, intended to understand how climate information is transferred through the karst system and archived in speleothems.

The air temperature inside the cave is around 7 °C, with slight differences between the upper and lower parts of the main passage. Relative humidity measurements were hampered by condensation on the capacitive sensors we used, thus we consider it to be close to 100%. The local meteoric water line ($\delta^2\text{H} = 7.7 \delta^{18}\text{O} + 10.1$), constructed using monthly aggregated rainfall samples, is similar to the global one, revealing the Atlantic as the strongly dominant vapor source. The $\delta^2\text{H}$ excess values, as high as 17 ‰, indicate that precipitation has an important evaporative component, possibly given by moisture recycling over the European continent. CO₂ concentrations in cave air have a seasonal signal, with summer minima and winter maxima. This might be indicative of an organic matter reservoir deep within the epikarst that continues to decompose over the winter, possibly modulated by seasonal differences in cave ventilation. The maximum values of CO₂ show a rise after the summer of 2014, from around 2000 ppm to about 3500 ppm. An analogous rise is seen in drip water stable isotopes and chemical elements such as Sr and Mg. The variability of stable isotopes and chemical elements is similar at all points inside the cave, indicating that they are draining a homogenous reservoir. Using two newly designed types of water/air equilibrators we were able to determine drip water dissolved CO₂, by measuring its concentration in the equilibrator headspace and then using Henry's law to calculate its concentration in water. This opens the possibility of continuous data logging using infrared technology without the need of costly and less reliable chemical determinations.



1. Introduction

The large-scale monitoring of karst systems is mainly undertaken from the perspective of water resource management (e.g. White, 1988; Ford and Williams, 2013). However, the use of speleothems as tools for climate reconstruction requires monitoring at a much finer spatial and temporal scale, where water/rock and water/atmosphere interactions have to be taken into account. With the knowledge that individual karst systems and even individual speleothems within a cave respond differently to environmental change, came the need for a better understanding of these behaviors. Lately, a series of review papers have detailed the systematics of stable isotopes and chemical elements behavior (Lachniet, 2009; McDermott, 2004; Fairchild et al., 2006) while the book of Fairchild and Baker (2012) offers an updated and detailed framework for speleothem paleoclimatology.

One of the most used proxies for the study of the water cycle is $\delta^{18}\text{O}$ and, by extension, $\delta^2\text{H}$. The interpretation of speleothem $\delta^{18}\text{O}$ values is not usually straightforward because they are influenced by thermal and hydrological processes, sometimes in opposing ways. For example, the altitude effect could be counteracted by a rain shadow effect, as evidenced in the Andes by Chamberlain and Poage (2000). Vapor source of rainfall or conditions at the vapor source could be distinguished using $\delta^{18}\text{O}$ and $\delta^2\text{H}$ and represent an important part in speleothem paleoclimate reconstructions. These characteristics are usually inferred based on the meteoric water line and the d-excess values in precipitation or cave drip water (Craig, 1961; Gat, 1996; Pfahl and Sodemann, 2014). When entering the soil-karst system, water can be subjected to evaporation in the soil, the epikarst or even in the cave before calcite deposition, thus imprinting higher values to calcite than the original rainfall (Dumitru et al., 2016; Markowska et al., 2016).

While drip water $\delta^{18}\text{O}$ can be modified by evaporation, another important proxy, $\delta^{13}\text{C}$, can be kinetically altered by strong degassing of CO_2 from solution when the gradient between drip water $p\text{CO}_2$ and cave atmosphere $p\text{CO}_2$ is large (Hendy, 1971; McDermott, 2004). CO_2 concentration in cave air is generally a result of soil CO_2 input, modulated by cave ventilation (Atkinson, 1977; White, 1988). Higher concentrations of dissolved CO_2 follow enhanced plant respiration and organic matter decomposition in the soil and thus, dissolved CO_2 in cave waters gives an estimate of soil organic activity. Compared against cave air CO_2 , it helps identify variations in cave ventilation, periods with increased calcite deposition or with increased kinetic fractionation of $\delta^{13}\text{C}$ (Banner et al., 2007; Matthey et al., 2010; Spötl et al., 2005). At present, dissolved CO_2 is usually modeled based on the alkalinity and pH of water (Spötl et al., 2005; Tooth and Fairchild, 2003; Riechelmann et al., 2013), but this approach is time consuming, costly, and offers only spot values.

Concentrations and ratios of certain elements (i.e. Mg/Ca, Sr/Ca) can reveal the interaction between water and the host rock. In some settings, Mg/Ca and Sr/Ca values were shown to be directly correlated with infiltration rates (Tooth and Fairchild, 2003) while in others they are inversely correlated, mediated by calcite precipitation prior to the drip site (Karmann et al., 2007), but also with calcite growth dynamics (Huang and Fairchild, 2001).

Here we present the results of an ongoing monitoring study started in 2012 which includes a set of parameters in both the water and the air at Ascunsă Cave and, for comparison, at Isverna Cave, the main collector of the karst system (Drăgușin et al., 2014). The region is very important from the climate point of view, as it lays at the intersection of Atlantic, Mediterranean and East European/West Asian air masses. Thus, better knowledge of present day changes would help in characterizing baseline conditions for this complicated interplay. This paper focuses more on stable



isotopes (H and O) and CO₂, while a forthcoming study will offer more insight into the behavior of chemical elements in drip water and farmed calcite. Our aim is to understand how environmental signals are transferred from the surface and how they are archived by speleothems, in order to understand speleothem proxies from this cave.

2. Materials and methods

5 Ascunsă Cave is situated in the Mehedinți Mountains (SW Romania), a region under a temperate-continental climate with Mediterranean influences (Bojariu and Paliu, 2001; Apostol, 2008; Baltă and Geicu, 2008). The cave is 671 m long, 145 m deep and its entrance is located at 1080 m above sea level (a.s.l.). This active cave, rich in speleothems, is developed mostly on the contact between wildflysch (mélange) and limestone. A small river enters the main cave passage at the White Chamber coming through the Tributary Passage, while and outside river was draining inside the
10 cave through the entrance. At the moment, the outside river is redirected along the valley and does not enter the cave anymore. Since 2012, a monitoring program was started and continuously developed at Ascunsă and Isverna caves, the latter situated at an altitude of 450 m a.s.l. and functioning as the main collector of this karst system.

Inside Ascunsă Cave, several sites were monitored (Fig. S1, Suppl. Mat.): POM Entr. (25 m from entrance, -7 m below the entrance level), POM A (100 m from entrance, -30 m), POM 2 (220 m from entrance, -80 m) and POM B (270 m from entrance, -90 m). Apart from these, we have also monitored the small river inside the cave, at a point close to
15 POM A, as well as the outside temperature.

In Isverna Cave, a temperature logger was placed at ~200 m from entrance in the Intermediary Passage, sheltered from the possible influence of the large river flowing through the lower level of the cave. Air temperature, rainfall amount and the isotopic composition of precipitation were also monitored close to the cave (460 m a.s.l.).

20 2.1. Air temperature and relative humidity

In 2014, Tinytag Plus2 temperature and relative humidity loggers were added to the monitoring setup. The logger that records outside temperatures at Ascunsă Cave (POM Ext.) was first placed in a fissure in the entrance area and then moved in December 2014 a few meters outside into another fissure and covered with litter. For this reason, the temperature recorded by it are only estimates for atmosphere values; however, they better reflect conditions at the
25 surface/subsurface interface.

Relative humidity in the two caves was difficult to measure for long periods of time. Condensing water vapor appears to saturate the sensors of data loggers, therefore we would consider RH to be close to 100 % at the two caves.

2.2. Rainfall amount, rain water and drip water stable isotopes

Rainfall amount was measured at Isverna village (460 m a.s.l.) using a Pluvimate rainfall logger. It should be taken
30 into account that the rainfall logger is not optimized to measure snow fall and can only measure the water produced by melting snow already present in its funnel. Rain water was collected in the same place in a 5 L volume primed with white paraffin oil to prevent evaporation.

H-O stable isotopes were measured in rainfall and drip waters using CRDS systems. For the period July 2012 - September 2013 they were measured at the Babeş-Bolyai University Stable Isotope Laboratory with a precision of



0.03‰ for $\delta^{18}\text{O}$ and 0.1‰ for $\delta^2\text{H}$. Reproducibility between measurements of duplicate samples was $\sim 0.08\%$ for $\delta^{18}\text{O}$ and $\sim 0.19\%$ for $\delta^2\text{H}$. All values are calibrated against VSMOW–SLAP.

Since September 2013 samples were measured at the Ștefan cel Mare University Stable Isotope Laboratory using a Picarro L2130i, coupled to a high precision vaporizer. Samples were manually injected in the vaporization chamber and the average of the last four injections for which the standard deviation was better than 0.02 for $\delta^{18}\text{O}$ and 0.2 for $\delta^2\text{H}$ was used in calculating the isotopic values. The raw values were normalized to the SMOW-SLAP scale using two internal standards (and a third one used as a control), the precision being better than 0.02 ‰ for $\delta^{18}\text{O}$ and 0.2 ‰ for $\delta^2\text{H}$.

To investigate the possible vapor sources, we modeled the back trajectories of air masses that were present at our site during days with rainfall above 5 mm. We ran the Hysplit 4 model (Draxler and Hess, 1997; Draxler and Hess, 1998; Draxler, 1999; Stein et al., 2015) using the GDAS 0.5° data for the coordinates of the pluviometer (44° 58' 48.26" N 22° 37' 15.13" E) at an altitude of 500 m above ground level.

2.3. Cave air CO₂

During our monitoring program we measured CO₂ concentration in the cave atmosphere at roughly two months intervals. CO₂ concentration was measured since July 2012 using two Vaisala GMP222 probes with an accuracy of (1.5 % of range + 2 % of reading). Between July 2012 and December 2014 we used a probe calibrated for the range 0-2000 (2k) ppm. Since December 2014, a GMP 222 probe calibrated for the range 0-10000 (10k) ppm was used. Because in October 2014 we measured values as high as 3560 ppm, larger than the 2000 ppm calibrated range of the probe, we ran a standardization experiment using the two probes. Following this test we saw that the 2k probe can confidently measure samples up to 3200 ppm. The errors associated with this figures are 221 ppm for the 10k and 97 ppm for the 2k, giving us confidence that the field measurements are genuine.

2.4. Drip water CO₂

To study drip water pCO₂ we adapted the headspace method that is typically used to measure gases evolving from open waters or soils (see for example (Broecker and Takahashi, 1966). Here we used two types of water/air equilibrators in which drip water was collected from stalactites via a tube and allowed to degas without having contact with the cave atmosphere (Fig. 1). Being isolated from the cave atmosphere, the CO₂ concentration values of the confined atmosphere (pCO_{2ca}) are considered to be in equilibrium with those of the confined drip water (pCO_{2cw}), following Henry's law. The confined atmosphere evolved from degassing of the accumulated water was sampled and the concentration of CO₂ was measured using a Vaisala GMP222 probe. As CO₂ concentration values are affected by temperature and atmospheric pressure, these parameters were measured with a Vaisala HMP70 temperature probe and a barometer (± 5 hPa resolution).

For the sampling itself, the GMP 222 probe was placed in a small volume attached to the equilibrator through a three-way closed valve. The probe volume was vacuumed using a manual vacuum pump also attached to the valve and, after checking the stability of the vacuum to insure no leakage and contamination with atmospheric air, the valve was



opened to allow air from the headspace to enter the probe volume. Throughout this time the handheld meter was turned off. After allowing enough time for the air sample to penetrate the probe's membrane, the handheld meter was turned on.

Type A equilibrator (Fig. 1, left) is comprised of two main parts: an inner cylinder which is open at the base, and a slightly wider, outer cylinder which is open at the top and hosts the inner cylinder. Water accumulated in the inner cylinder drains through its bottom and then flows upwards towards the rim of the outer one, where it drains. This insures that water accumulated from drips has a large surface that is opened only to the interior of the inner cylinder and degasses towards the headspace. In order to reduce CO₂ diffusion between cave air and the confined atmosphere through the accumulated water, the distance between the inner and outer cylinders has to be minimal, thus reducing the surface exposed towards the cave atmosphere. The rim height of the outer cylinder controls the height of the water table, and thus the headspace volume inside the inner cylinder. The headspace volume is important in relation with the sample quantity needed for the measurement, if the measurement is done on grab samples.

Type B equilibrator (Fig. 1, right) is simpler, accumulating water in a single volume and draining it through a tube mounted in its lower part. The upper level of this tube controls the water level inside the volume. In practice, we used a very long tube coiled around the exterior of the volume. The extended length of the tube has the role of hindering CO₂ degassing towards the cave atmosphere, thus maximizing the likelihood that the confined atmosphere remains in equilibrium with drip water.

When placing the equilibrators, care was taken in order for them to tap a stalactite with a high enough drip rate that would allow for the confined water to be constantly refreshed. Thus, we tried to reduce the danger of CO₂ mobility through the whole water mass either towards or from the cave atmosphere.

2.5. Cave water and farmed calcite chemistry

Drip water, pool water and river water were sampled from the White Chamber, POM A, POM 2 and POM B. We use the term drip water for samples that were allowed to drip directly into sampling vials, but also for those retrieved from the equilibrators described above.

A range of physical and chemical parameters were measured in the field. Using a WTW Sentix 41 electrode we measured the temperature and pH of cave waters, the latter after calibration with two buffer solutions with values of 7 and 10 that were left to equilibrate with the cave temperature. Electrical conductivity (EC) was measured using a WTW TetraCon 325 EC electrode. Total carbonate hardness was determined by titration using a Merck MColorstest water hardness test.

Water samples were collected and stored in Nalgene HDPE bottles. Samples for cation analysis have been filtered by using Thermo Scientific Chromacol Polyether Sulphone Syringe Filters (0.45 µm pore size). Suprapur (Merck) 65% nitric acid was used for pH adjustment of the samples. The complete chemical analysis of all water samples was conducted in the Hydrogeochemistry Laboratory of the Emil Racoviță Institute of Speleology, Bucharest. The concentrations of all elements considered here have been measured on a Perkin Elmer NexIon 300S Q-ICP-MS as follows: Mg and Sr in collision mode using Kinetic Energy Discrimination; Ca using the Dynamic Reaction Chamber



technique. All determinations were conducted in compliance with the US-EPA 6020B method (EPA, 2014). Calibrations were checked against NIST 1640a and NIST 1643e water standards. Chemical analysis of modern calcite was performed on the same Q-ICP-MS, after acid digestion, with NIST 1d (limestone, Argillaceous) as standard reference material.

5

2.6. Modern calcite stable isotopes

Calcite was precipitated on glass plates and was analyzed for O and C stable isotopes. Results for the period prior to April 2013 were reported by (Drăgușin et al., 2014). Calcite formed after this period was measured at CEA-CNRS-LSCE (France) on a VG-OPTIMA mass spectrometer. For each analysis, around 100μg of calcite powder was reacted with phosphoric acid at 90 °C and, after cryogenic separation, the resulting CO₂ was measured relative to a reference gas that has been calibrated against a series of isotopic standards.. All values are reported in ‰ relative to the VPDB. The error is better than 0.08 ‰ for δ¹⁸O and 0.05 ‰ for δ¹³C

10

3. Results and discussion

3.1. Temperature regime of Ascunsă and Isverna caves

For a better comparison we use here data logged continuously between February 2015 and February 2016, when all the logs overlap. The external temperature at the two caves has a good correlation, with Ascunsă values showing lower daily amplitude, related probably to its subsurface location and in a forested area. The mean value over this period was 6.91 °C (SD=6.48) at Ascunsă and 14.25 °C (SD=7.48) at Isverna. Using temperature values from the European Climate Assessment (ECA) (Klein Tank et al., 2002) for Drobeta Turnu-Severin meteorological station located approximately 40 km to the south at 77 m a.s.l. (average 14.00 °C, SD=9.24), we see that temperature in our area evolved together with regional ones (Fig. 2).

20

Based on the good agreement between our site and the Drobeta meteorological station, we could use data from the latter in order to get more insight into the relative temperature variability over the whole monitored period at our site. Annual temperature at Drobeta decreased from an average of 13.7 °C in 2012 to a value of 13.3 °C in 2014, only to rise to 14.1 °C in 2015 (Fig. S2, Supp. Mat.). At seasonal scale, we see a more complex image. Average winter values increased constantly between 2012 (0.5 °C) and 2016 (4.6 °C), while spring temperatures generally decreased. Summer and autumn values were coupled, both showing a decrease between 2012 and 2014, and a rise in 2015 which resembles the variability of annual temperature. Thus, it appears that the summer/autumn couple controls the annual temperature values.

25

At Ascunsă Cave, POM2 and POM A have a stable temperature regime (Fig. S3, Supp. Mat.). While the average at POM2 is 7.29 °C (SD=0.05) at POM A it is 7.04 °C (SD=0.06). At the same, time POM Entr. shows higher variability (average 5.84 °C, SD=0.72) due to its proximity to the entrance and to the steep morphology of the passage, which allows cold air to easily reach this point. Inside Isverna Cave the average temperature was 10.06 °C (SD=0.02). Because the variability at POM A and POM 2 is so small and would not affect any isotopic calculations that could be

30



performed, we will not discuss it further. We only note that between May 2015 and November 2015 the temperature at the three points inside Ascunsă Cave showed a steady increase, while over the following winter they show a slight decrease interrupted by brief minor “cold spells”. At POM A this behavior is different than during the 2014-2015 winter, when the logger recorded stronger cooling (~ 0.15 °C). At POM 2 the two winter signals have similar
5 amplitude. At Isverna too, the winter variability is around 0.05 °C but the summer of 2016 records a steady 0.25 °C warming, much stronger than the -0.05 °C recorded during the 2015 summer.

Given a 2.8 °C difference between Isverna and Ascunsă (POM 2), we could calculate a local lapse rate of 6.1 °C km^{-1} , in agreement with the global value of 6.4 °C km^{-1} (Brunt, 1933) that should be taken into account when discussing the altitude effect on $\delta^{18}\text{O}$.

10

3.2. Drip rate variability

Drip rate at POM 2 shows a generally decreasing trend between August 2014 and October 2015, in accordance to a decrease in rainfall amount (Fig. 3). After a period of pluvial events in October 2015, the general values rose higher than at the start of the logging period but recorded another long term decrease until present. This general variability is
15 punctuated by high drip rates linked to rainfall events. The quick response of the drip rate to rainfall indicates a fracture recharge of the karst system (White, 2002; Ford and Williams, 2013). On the other hand, the good correlation with rainfall amounts from Isverna and Drobeta could be used for the instrumental calibration of proxies linked to drip rate, based on the fact that the Drobeta dataset goes back to 1925.

3.3. CO₂ concentration in cave air and drip water

20 The variability of cave atmosphere CO₂ (CO_{2atm}) at POM Entr. is in close relation with outside temperatures, reaching 2500 ppm during the warm season but only 500 ppm in winter (Fig. 4). This might reflect a seasonal input of soil derived CO₂ which is stronger in summer and weak during the cold season, combined with stronger winter ventilation. Air temperature at this site is between 5 and 7 °C during summer, much colder than outside air, and between 4 and 6 °C during winter, warmer than outside air. The winter setting could lead to stronger convective air circulation
25 (Fairchild and Baker, 2012), efficiently ventilating the entrance part of the cave. The winter mode is shorter than the summer one, covering the period November - December to March - April, and the transition between the two is sharp. At the other three monitoring sites inside Ascunsă Cave, CO_{2atm} records show similar trends: high values in October and low in April. The CO₂ concentrations vary between 700 and 2100 ppm over the period July 2012 to July 2014 but rose following the summer season of 2014 and reached a maximum of 4040 ppm in March 2016. While the higher
30 CO_{2atm} recorded during 2014-2016 could be easily explained by enhanced biological activity following the temperature increase, we cannot rule out a possible weakening ventilation.

Even though limestone thickness is different between the upper and the lower parts of the cave, the CO_{2atm} signal remains the same. This striking resemblance could be due to similar transfer times of soil CO₂ through the epikarst and karst and to similar ventilation processes throughout the cave.

35 Although the production of soil CO₂ peaks in the warm season (Lloyd and Taylor, 1994; Breecker et al., 2012), the fact that we recorded the highest CO_{2atm} values in winter could represent a delay in transferring the signal from surface.



However, as drip water $\delta^{18}\text{O}$ suggests that the transfer time of water is on the order of days, this delay might mean that most of the cave $\text{CO}_{2\text{atm}}$ comes in gas form mostly via open fissures on longer timescales and is not entirely a result of degassing of drip water inside the cave. An alternate explanation would be that there are regions of CO_2 production deep within the epikarst, as theoretically proposed by Atkinson (1977) and later suggested by Matthey et al. (2010) at New St. Michael Cave in Gibraltar. This possibility seems to be supported by the observation of a ventilation event in January 2016 which was expressed at all three inner sites as a ~ 1000 ppm reduction in CO_2 concentration following a drop of 10°C in outside air temperature. Together with the subsequent rise in values, this event reveals the role of ventilation in $\text{CO}_{2\text{atm}}$. Besides, it also implies that there is a steady CO_2 flux towards the cave, compatible with a winter production deep within the karst system.

The concentration of CO_2 in infiltrating waters ($\text{CO}_{2\text{cw}}$) was calculated using Henry's law, based on the values measured in the confined atmosphere of the equilibrator headspace ($\text{CO}_{2\text{ca}}$) and considering the solubility of CO_2 in water ($H^{\text{c}}=c_{\text{cw}}/c_{\text{ca}}$) as 0.83 (Sander, 2015). In Fig. 5 we see that, with no exception, $\text{CO}_{2\text{ca}}$ (and, by extension, $\text{CO}_{2\text{cw}}$) was always greater than $\text{CO}_{2\text{atm}}$ by a few thousand ppm. Nevertheless, as opposed to $\text{CO}_{2\text{atm}}$, $\text{CO}_{2\text{ca}}$ shows differences between the three sites. At POM A $\text{CO}_{2\text{ca}}$ has the highest values, reaching over 11000 ppm, close to theoretical concentrations in soil atmosphere (Atkinson, 1977 and references therein; Brook et al., 1983), and shows a similar profile to $\text{CO}_{2\text{atm}}$. POM 2 has slightly lower values, while POM B recorded the lowest values of the three points. This different behavior shows that the CO_2 input via drip water is not similar throughout the cave and suggests that there are either different sources of CO_2 feeding the system or different pathways toward these drip sites. The ventilation event of January 2016 appears to have slightly affected POM A $\text{CO}_{2\text{ca}}$ too, indicating that ventilation occurs at some extent on the CO_2 pathway to this site.

An interesting feature is observed as POM 2 and POM B $\text{CO}_{2\text{ca}}$ appear to be inversely correlated. They seem to complete a full year cycle of diverging away and back to each other with the end points of this cycle situated in March 2015 and March 2016. We suggest that understanding this behavior might be useful, accompanied by more observations, for the calculation of CO_2 fluxes between different sectors of the karst system.

This difference observed between $\text{CO}_{2\text{cw}}$ and $\text{CO}_{2\text{atm}}$ is also seen between the modeled partial pressure in pool waters ($\text{pCO}_{2\text{fw model}}$) that are considered to be in equilibrium with the cave atmosphere and the modeled pCO_2 of the confined water ($\text{pCO}_{2\text{cw model}}$) calculated using the PHREEQC program (Fig. S4a, Supp. Mat.). Nevertheless, the modeled values of the confined water are different, at times, from those based on the direct measurements ($\text{pCO}_{2\text{cw measure}}$) (Fig. S4b, Supp. Mat.). This might be due to a range of uncertainties inherent from the different physical and chemical measurements of cave waters that were not considered here (e.g.: the determination of hardness or alkalinity by titration or the determination of pH). Using only the measured $\text{pCO}_{2\text{ca}}$ to calculate $\text{pCO}_{2\text{cw}}$ limits the intervening errors just to the straightforwardly known measurement error and to that associated with the empirical determination of Henry's law constant.

In support of the robustness of the method used here, apart from pCO_2 there is a visible difference in the pH of the confined water (pH_{cw}) and the pool water (pH_{fw}), with pH_{cw} always having lower values (Fig. S5a, Supp. Mat.). A clear difference is also seen in total carbonate hardness and electrical conductivity, with confined waters having always



greater values in both parameters (Fig. S5b and c, Supp. Mat.). These differences could be explained by the higher content of dissolved CO₂.

3.4. Rain and drip water stable isotopes

3.4.1. Rainfall isotopic signature

- 5 Between September 2014 and June 2016 $\delta^{18}\text{O}$ values in precipitation show seasonal variability, between a minimum of -14.68 ‰ in January 2016 and a maximum of -4.75 ‰ in April 2015 (Fig. 6). The weighted average $\delta^{18}\text{O}$ and $\delta^2\text{H}$ values of January-December 2015 are -9.36 ‰ and -62.09 ‰, comparable to weighted annual means derived from GNIP (IAEA/WMO, 2016). During 2015, weighted averages at Drobeta were -8.31 ‰ and -53.56 ‰, respectively.
- 10 The Local Meteoric Water Line (LMWL) at Isverna is defined as $\delta^2\text{H}=7.7\delta^{18}\text{O} + 9.7$, for January - December 2015, and $\delta^2\text{H}=7.7\delta^{18}\text{O} + 10.1$ for September 2014 to June 2016, an equation similar to the global meteoric water line (GMWL (Craig, 1961). At Drobeta, the 2015 LMWL is defined as $\delta^2\text{H} = 7.9\delta^{18}\text{O} + 9.5$ and d-excess values varied between 4 and 16 ‰ (Fig. S6a, Supp. Mat.).
- While we would expect a Mediterranean contribution to precipitation brought via the winter cyclones (Bojariu and Paliu, 2001), the LMWL equation seems to indicate the Atlantic Ocean as a heavily dominating vapor source.
- 15 Knowing that the equation of the Mediterranean meteoric water line is $\delta^2\text{H} = 8\delta^{18}\text{O} + 22$ ‰ (Gat and Carmi, 1987), any mixing of the two sources would modify the LMWL.
- The d-excess values fall between 11 and 15 ‰, outside the range predicted by GNIP and characteristic of a region with enhanced evaporation (Dansgaard, 1964; Gat et al., 2003; Delattre et al., 2015). At Drobeta they have similar values and variability (Fig. S6b, Supp. Mat.), indicating a regionally consistent setting.
- 20 Between August 2014 and August 2016 there were 104 rainy days with at least 5 mm of rain and we modeled the five day back trajectories of the air masses present at our site during these days (Fig. 7). These trajectories appear to fall within four categories: Atlantic, Mediterranean, E European/W Asian and a more local one, not spreading much outside the Carpathian-Balkan region. Nevertheless, it can be seen that some of the East European trajectories are in fact deflections of Atlantic pathways. Thus, the majority of the air masses arriving at our site during rainy days appears
- 25 to be of Atlantic origin, with only a restricted number originating in the Mediterranean. As the origin of an air mass is not definitive evidence for the origin of moisture that condensed when it arrived at our site, it is still an indication of the vapor source. We note that it is not within the scope of this paper to detail the exact moisture content of each air mass whose trajectory we modeled, but that it should be the aim of further study. As we see that the Mediterranean was a minor contributor to local precipitation, the evaporative component implied by the d-excess could indicate that
- 30 rainfall included an important element of recycled moisture over the European land-mass (Aemisegger et al., 2014). In December 2015 an unusually high $\delta^{18}\text{O}$ value of -9.04 ‰ was recorded. Throughout the whole month, we recorded a single rain episode of 6 mm on 01 December 2015. This event started in the afternoon when the air temperature was 12 °C and ended at midnight when temperatures were still as high as 9 °C. The air mass present at our site during this day appears to have travelled through Central Europe, across the Adriatic and into the Thyrrhenian Sea, from where it
- 35 returned to mainland Europe. This complicated pathway makes the air mass prone to accumulate both continental and



Mediterranean moisture. We suggest that the high isotopic value is also linked to the abnormally high air temperature for this season that promoted higher continental evaporation and is not representative for seasonal variability.

3.4.2. Drip water stable isotopes

5 At Ascunsă Cave drip water $\delta^{18}\text{O}$ shows almost the same variability at all sites (Fig. 8). A similar variability is seen in drip water at the Green Lake in Isverna Cave too, although here the values are higher, an expected result of the altitude effect. This gives us confidence that this signal at Ascunsă Cave is not site related and that it is indeed representative for the surrounding area. Drip water $\delta^{18}\text{O}$ at the two caves rose in the summer of 2014. For example, at
 10 POM2 the 2012-2014 average $\delta^{18}\text{O}$ was -10.65‰ , whereas the following period had an average of -10.19‰ . Here, the 2012-2016 water line is defined as $\delta^2\text{H} = 5.0\delta^{18}\text{O} - 16.8$ (Fig. 9a). For the period August 2013 – August 2016, drip water at the Green Lake in Isverna Cave has a water line defined as $\delta^2\text{H} = 6.1\delta^{18}\text{O} - 5.2$ and d-excess values around 12-13 ‰, with an exception in September 2014, when we recorded 7.95 ‰.

The September 2014 values and, at other drip sites, those from August 2014 too, have an outlier character in both $\delta^{18}\text{O}$ and $\delta^2\text{H}$. On 17 August we measured values as high as -9.62‰ at POM 2, while on 17 September we measured -9.18
 15 ‰. Compared to the whole d-excess record at POM 2 which runs between 13 and 16 ‰, their values stand out for being very low (9.5 and 6.8 ‰, respectively). Such anomalous values, recorded at all drip sites appear to be linked to the advection of air masses from around the Caspian Sea (Fig. 7). For that region, the weighted August and September $\delta^{18}\text{O}$ values stand between -6 and -2‰ and the weighted d-excess around 0 (IAEA/WMO, 2016). Such an enriched moisture source would explain both the $\delta^{18}\text{O}$ and d-excess values recorded during these events. After discarding the
 20 enriched values of August and September 2014 but also those of March 2015, the ground water line (GWL) at POM 2 is $\delta^2\text{H} = 7.9\delta^{18}\text{O} + 13.6$ and d-excess values fall between 13 and 15.5 ‰. At the Green Lake, after discarding the September 2014 values, the GWL becomes $\delta^2\text{H} = 8.0\delta^{18}\text{O} + 12.7$.

The September 2014 event, with $\delta^{18}\text{O}$ values as high as -8.72‰ , is replicated in both caves, and follows a high intensity precipitation episode that took place a week prior. At Drobeta it peaked at a total of 157 mm on 14 and 15
 25 September 2014, while at Isverna we recorded 104 mm during these two days. The study of these two rain events and their reflection in the cave is interesting from two points of view: first of all it indicates that the transfer time of water from surface to the cave is on the order of days. Secondly, the lack of any strong peaks in the drip log at this time could be assigned to the fact that they did not contribute too much to reservoir recharge. At POM 2, a declining trend was present before the September event, probably associated with summer drought. On 18 September 2014, three days
 30 after the rain event, the drip rate started to rise from 28 drips min^{-1} and peaked two days later at only 31 drips min^{-1} . For comparison, a rain event from 22-23 October 2014 totaling 116 mm produced a rise in drip rate from 21 to 90 drips min^{-1} . This was followed by a long period when drip rates remained above 30 drips min^{-1} .

After discarding the August-September 2014 values, we recalculated the groundwater lines from our drip sites and compared them to the LMWL. From Fig. 9b we can see that they all have intercept values above 10. This could be
 35 due to processes that take place after the precipitation reaches the ground, most probably evaporation in the soil/epikarst. We can also see that the GWL at the Green Lake inside Isverna Cave is closest to the LMWL, while all the Ascunsă Cave plot the highest.



3.5. Cave water chemistry

The chemical composition of water shows a similar behavior at all points (Fig. S7, Supp. Mat.), suggesting that they are draining a single, well-mixed reservoir, an indication similar to that of the stable isotopes.

Calcium concentrations as low as 29 mg L⁻¹ appear during the 2012-2013 winter but also during the summer of 2014.

5 The highest concentration was recorded in March 2015, when values peaked at 119 mg L⁻¹. Magnesium concentrations are clearly different between the three inner monitoring sites, with POM B having the highest concentrations while POM A has the lowest ones. They also seem to have a seasonal variability over 2014-2015. Concentrations as low as 0.37 mg L⁻¹ were recorded in the pool waters of POM A in September 2013 but were usually around 0.8 mg L⁻¹.
10 Following a wetter period between 07 and 19 October 2015, the values rose to 1.21 mg L⁻¹ and remained high later into November 2015. Strontium concentrations show an important transition towards higher values following the summer of 2014, from around 0.030 mg L⁻¹ to a maximum of 0.057 mg L⁻¹. Values remained high until the pluvial events of October 2015, when they dropped to as low as 0.02 mg L⁻¹. The competing signals recorded in the autumn and winter of 2015-2016 by Mg and Sr induced a strong signal in the Sr/Ca and Mg/Ca values too.

15 Although the chemical records at these drip sites cover almost three years, the large fluctuations of Mg and Sr hinder our attempts at drawing any definitive conclusion on the processes responsible for their variability. For example, the covariation of Sr/Ca and Mg/Ca is seen as a sign of prior calcite precipitation (Fairchild et al., 2000), but their different response to the pluvial events mentioned above requires the interference of other processes. A forthcoming paper discussing the in-depth chemistry of Ascunsă Cave will try to clarify some of these aspects.

3.6. Farmed calcite geochemistry

20 3.6.1. Stable isotopes

Average $\delta^{18}\text{O}$ values of farmed calcite at POM 2 (-8.07 ‰) and POM X (-7.88 ‰) show similar variability throughout the monitored period, with the POM X samples having, in general, higher values (Fig. 10). These could be a consequence of the observed slower drip rate that could have resulted in a stronger degassing of the water droplets and film, which in turn led to stronger kinetic fractionation. Using the equations of Kim and O'Neil (1997) and
25 Tremaine et al. (2011) we calculated the theoretical $\delta^{18}\text{O}$ equilibrium values of the farmed calcite at POM2 and POM X, at 7.2 °C. The input value for drip water $\delta^{18}\text{O}$ was considered as the average of samples bracketing the farming period. The measured $\delta^{18}\text{O}$ values plot above the Kim and O'Neil (1997) predictions and below those predicted by the equation of Tremaine et al. (2011). On average, the measured values are 0.6 ‰ more depleted compared to those calculated using the Tremaine et al. (2011) equation, while they are ~0.4 ‰ more enriched than those predicted by
30 Kim and O'Neil (1997).

For the deposition period June-August 2014 we used the drip water $\delta^{18}\text{O}$ at the beginning of the interval, as the enriched drip water from August 2014 would predict an unreasonable value of -6.77 ‰ / -7.70 ‰.

The POM X $\delta^{13}\text{C}$ values appear to be affected too by the slow drip rate and the increased kinetic fractionation that accompanies it. The values are higher than at POM2 and more variable. When compared to the available drip rate
35 recorded at POM2, we see that two low $\delta^{13}\text{C}$ values (-10.54 ‰ and -11.03 ‰) occur during periods with average drip rates of 33 and 43 drips min⁻¹ respectively (September/December 2014 and December 2014-February 2015), while a



third one (-9.65 ‰), was measured from a period with an average of 13 drips min⁻¹ (July-August 2015). The higher isotopic values recorded during low discharge hint towards enhanced kinetic fractionation.

Moreover, when POM X $\delta^{13}\text{C}$ values are compared with average air temperatures from Drobeta (ECA dataset, Klein Tank et al., 2002), there is a good correlation between the two ($r = 0.52$), except for two periods: November 2012 -
5 February 2013 and August - September 2013. If these two samples are omitted from the calculation, the correlation coefficient is 0.92. We note that we also calculated the precipitation amount for the same periods and their correlation with $\delta^{13}\text{C}$ or $\delta^{18}\text{O}$ is weak. The same test was applied for POM2 farmed calcite and it showed a lack of correlation.

A direct correlation between calcite $\delta^{13}\text{C}$ and outside air temperature is counterintuitive, as common knowledge states that warmer periods are characterized by lower calcite values due to the input of more depleted $\delta^{13}\text{C}$ via organic
10 activity (see for example the review of McDermott, 2004). Such a direct correlation could be induced by a full seasonal delay in the transfer time of the surface signal, but this is contradicted by the common variability of $\delta^{18}\text{O}$ at both POM 2 and POM X. Besides, as this $\delta^{13}\text{C}$ anomaly is not replicated at POM 2, it could mean that it is a process specific to POM X. A likely explanation would be that it is the result of kinetic fractionation during periods with increased pCO₂ gradients between drip water and cave atmosphere, a process further enhanced by low drip rates. Assuming that higher
15 air temperature is transposed into higher drip water CO₂, we calculated, for the periods with available $\delta^{13}\text{C}$ data, average air CO₂ at POM 2 as well as the average temperature values from Drobeta. Further, we normalized the resulting values and subtracted CO₂ from temperature. We then plotted the resulting values in Fig. 11, considering that larger differences represent steeper CO₂ gradients between drip water and air, while lower differences represent gentler gradients. We can see that there is good correlation between the two data sets, except for the periods November
20 2012 – February 2013 and August – September 2013. If these two samples are omitted from the calculation, the correlation coefficient is 0.73.

While the two stalagmites have similar $\delta^{18}\text{O}$ behaviors, the POM X $\delta^{13}\text{C}$ might prove helpful in extracting information on the past kinetic fractionation strength and its controls: cave air CO₂/ventilation and drip water CO₂/outside temperature.

25 3.6.2. Chemical elements

The variability of chemical elements and ratios of calcite farmed at POM X is more expressive than at POM 2, and we will focus here only on them. In Fig. S8 (Supp. Mat.) we compare the measured calcite values against those of drip water from POM 2 and against the precipitation amount at Drobeta. Calcium values appear to correlate positively with those of the drip water, indicating that the signal is reliably transferred between water and calcite. The correlation with
30 rain amount is negative in August 2013 and August 2015, but positive in April-June 2014 and October-December 2014. Mg and Mg/Ca have a negative and stronger correlation with rain amount than with drip water values, while Sr and Sr/Ca show a negative correlation with drip water but a positive one with rain amount for three of the four points.



4. Concluding remarks

We presented a series of chemical and physical parameters recorded in air, water and modern calcite at Ascunsă and Isverna caves in SW Romania over the period 2012-2016. By comparison with data from the Drobeta meteorological station, we showed that precipitation and air temperature outside of the two caves fit within the regional setting.

5 Monthly collected rain water had in 2015 a weighted mean of -9.36 ‰, comparable to weighted annual means of this region derived from GNIP data. From the full dataset we discern a clear seasonal signal of $\delta^{18}\text{O}$, with winter values as low as -15 ‰ and summer values as high as -4 ‰. The local meteoric water line is equal to the global one and $\delta^2\text{H}$ excess values are as high as 16 ‰, much higher than those interpolated from GNIP, which lacks any long term data from Romania. Modelling of back trajectories shows that most of the air masses that were present at our site during
10 rainy days are of Atlantic origin, with reduced input from the Mediterranean. This suggests that the elevated $\delta^2\text{H}$ excess values are mostly the result of Atlantic moisture being recycled over the European continent.

$\delta^{18}\text{O}$ values and variability inside Ascunsă Cave are similar at all points, indicating that water at the monitored sites originates from a single, homogenous reservoir. Moreover, the variability is reproduced at Isverna Cave too, where $\delta^{18}\text{O}$ values are higher, as expected from the 600 m difference in altitude. After the warm season of 2014, values
15 increase at all points by about 0.5 ‰. Two enriched isotopic events in August and September 2014 indicate that water transfer time is on the order of days. Also, the drip rate logged inside Ascunsă Cave responds quickly to rainfall events, revealing a fracture flow type.

Carbon dioxide levels in cave air rose after the warm season of 2014, almost doubling their concentration from around 2000 ppm to about 4000 ppm. Using two specially adapted types of air/water equilibrators, we were able to measure
20 dissolved CO_2 concentrations in drip water, revealing different behaviors between the three monitored points. This behavior was not obvious in the cave air CO_2 concentrations, which shows that the underground atmosphere is well homogenized. These equilibrators helped us determine drip water CO_2 concentration (hence pCO_2) much easier than using the classical approach which relies on costly chemical analysis, strongly dependent on field measured pH and alkalinity and which only offers spot values. Our approach depends only on the direct measurement of CO_2 in the
25 headspace of the equilibrator and the subsequent calculation of water CO_2 using Henry's law. Thus, it opens the way to cost effective logging of cave water CO_2 that could be applied in speleothem science but also in show cave monitoring, where visitors are an important source of CO_2 . Moreover, these equilibrators could be used to sample any dissolved gas for concentration and stable isotopic measurements.

As in the case of stable isotopes, the Ca, Mg and Sr concentrations of cave waters are almost identical at all sites and
30 show the same variability, supporting the notion that these waters drain a single, homogenous reservoir. They also show an increase in value after the warm season of 2014, similar to stable isotopes and air CO_2 .

Modern calcite analysis showed that stalagmite POM X $\delta^{13}\text{C}$ is directly linked to outside temperatures via kinetic fractionation within the cave and could be used for the reconstruction of past kinetic effects at this site. This effect is not seen in the nearby POM 2 stalagmite. Moreover, the $\delta^{18}\text{O}$ of the two stalagmites shows similar variability and a
35 drip water fractionation function slightly different than those proposed by Kim and O'Neill (1997) or Tremaine et al. (2011).



The chemical signals are more successfully transferred to modern calcite from drip water especially at POM X, giving the possibility of using chemical proxies from this stalagmite to reconstruct past environmental changes.

Author contribution

- 5 V. Drăgușin designed the study, V. Drăgușin, S. Balan, I. Mirea, L. Tîrlă, M. Vlaicu performed fieldwork, V. Drăgușin and S. Balan designed the water/gas equilibrators, D. Blamart, V. Drăgușin F. L. Forray, I. Mirea, V. Nagavciuc and A. Perșoiu performed isotopic analysis, C. Marin and A. Tudorache performed chemical analysis, V. Drăgușin and L. Tîrlă modeled back-trajectories of air masses. V. Drăgușin prepared the manuscript with contributions from all co-authors. The authors declare that they have no conflict of interest.

10

Acknowledgements

- This study was financially supported by the following grants: IFA-CEA C4-08 (FREem, Co-PIs S. Constantin and D. Blamart), 17 SEE (CAVEMONITOR, PI S. Constantin), PN-II-RU-TE-2011-3-0235 (PI A. Perșoiu), PNII-RU-TE-2014-4-1993 (PI A. Perșoiu), 790/2014 (Co-PIs A. Perșoiu and D. Genty) and 18 SEE (PI C. Roibu). The authors gratefully acknowledge the NOAA Air Resources Laboratory (ARL) for the provision of the HYSPLIT transport and dispersion model used in this publication. We would also like to thank all our friends and colleagues who helped us during the last four years of fieldwork and especially to Emilian Isverceanu and his family for their continuous support.

15

References

- 20 Aemisegger, F., Pfahl, S., Sodemann, H., Lehner, I., Seneviratne, S. I., and Wernli, H.: Deuterium excess as a proxy for continental moisture recycling and plant transpiration, *Atmos. Chem. Phys.*, 14, 4029-4054, 10.5194/acp-14-4029-2014, 2014.
- Apostol, L.: The Mediterranean cyclones—the role in ensuring water resources and their potential of climatic risk, in the east of Romania, *Present environment and sustainable development*, 2, 143-163, 2008.
- 25 Atkinson, T. C.: Carbon dioxide in the atmosphere of the unsaturated zone: An important control of groundwater hardness in limestones, *Journal of Hydrology*, 35, 111-123, 10.1016/0022-1694(77)90080-4, 1977.
- Baltă, D., and Geicu, A.: Factorii dinamici ai atmosferei, in: *Clima României*, edited by: Sandu, I., Pescaru, V. I., Poiană, I., Geicu, A., Căndea, I., and Țăște, D., Editura Academiei Române, Bucharest, 38-56, 2008.
- Banner, J. L., Guilfoyle, A., James, E. W., Stern, L. A., and Musgrove, M.: Seasonal variations in modern speleothem calcite growth in Central Texas, U.S.A., *Journal of Sedimentary Research*, 77, 615-622, 10.2110/jsr.2007.065, 2007.
- 30 Bojariu, R., and Paliu, D. M.: North Atlantic Oscillation Projection on Romanian Climate Fluctuations in the Cold Season, in: *Detecting and Modelling Regional Climate Change*, edited by: Brunet India, M., and Bonillo, D. L., Springer, Berlin Heidelberg, 345-356, 2001.
- Breecker, D. O., Payne, A. E., Quade, J., Banner, J. L., Ball, C. E., Meyer, K. W., and Cowan, B. D.: The sources and sinks of CO₂ in caves under mixed woodland and grassland vegetation, *Geochimica et Cosmochimica Acta*, 96, 230-246, 10.1016/j.gca.2012.08.023, 2012.

35



- Broecker, W. S., and Takahashi, T.: Calcium carbonate precipitation on the Bahama Banks, *Journal of Geophysical Research*, 71, 1575-1602, 10.1029/JZ071i006p01575, 1966.
- Brook, G. A., Folkoff, M. E., and Box, E. O.: A world model of soil carbon dioxide, *Earth Surface Processes and Landforms*, 8, 79-88, 10.1002/esp.3290080108, 1983.
- 5 Brunt, D.: The adiabatic lapse-rate for dry and saturated air, *Quarterly Journal of the Royal Meteorological Society*, 59, 351-360, 10.1002/qj.49705925204, 1933.
- Chamberlain, C. P., and Poage, M. A.: Reconstructing the paleotopography of mountain belts from the isotopic composition of authigenic minerals, *Geology*, 28, 115-118, 10.1130/0091-7613(2000)28<115:rtomb>2.0.co;2, 2000.
- Craig, H.: Isotopic Variations in Meteoric Waters, *Science*, 133, 1702-1703, 10.1126/science.133.3465.1702, 1961.
- 10 Dansgaard, W.: Stable isotopes in precipitation, *Tellus*, 16, 436-468, 10.1111/j.2153-3490.1964.tb00181.x, 1964.
- Delattre, H., Vallet-Coulomb, C., and Sonzogni, C.: Deuterium excess in the atmospheric water vapour of a Mediterranean coastal wetland: regional vs. local signatures, *Atmos. Chem. Phys.*, 15, 10167-10181, 10.5194/acp-15-10167-2015, 2015.
- Drăgușin, V., Staubwasser, M., Hoffmann, D. L., Érsek, V., Onac, B. P., and Vereș, D.: Constraining Holocene hydrological changes in the Carpathian-Balkan region using speleothem $\delta^{18}\text{O}$ and pollen-based temperature reconstructions, *Climate of the Past*, 10, 1363-1380, 10.5194/cp-10-1363-2014, 2014.
- 15 Draxler, R. R., and Hess, G. D.: An overview of the HYSPLIT_4 modeling system of trajectories, dispersion, and deposition, *Australian Meteorological Magazine*, 47, 295-308, 1998.
- Draxler, R. R.: HYSPLIT4 user's guide, NOAA Tech. Memo. ERL ARL-230, NOAA Air Resources Laboratory, Silver Spring, MD, 1999.
- 20 Draxler, R. R., and Hess, G. D.: Description of the HYSPLIT_4 modeling system, NOAA Tech. Memo. ERL ARL-224, NOAA Air Resources Laboratory, Silver Spring, MD, 1997.
- Dumitru, O. A., Forray, F. L., Fornós, J. J., Ersek, V., and Onac, B. P.: Water isotopic variability in Mallorca: a path to understanding past changes in hydroclimate, *Hydrological Processes*, 10.1002/hyp.10978, 2016.
- 25 EPA, U.-. Method 6020B. Inductively Coupled Plasma - Mass Spectrometry. Revision 2, 2014.
- Fairchild, I. J., Smith, C. L., Baker, A., Fuller, L., Spötl, C., Matthey, D., and McDermott, F.: Modification and preservation of environmental signals in speleothems, *Earth-Science Reviews*, 75, 105-153, 2006.
- Fairchild, I. J., and Baker, A.: *Speleothem Science: From Process to Past Environments*, Wiley-Blackwell, Chichester, 416 pp., 2012.
- 30 Ford, D., and Williams, P. D.: *Karst hydrogeology and geomorphology*, John Wiley & Sons, 2013.
- Gat, J. R., and Carmi, I.: Effect of climate changes on the precipitation patterns and isotopic composition of water in a climate transition zone: Case of the Eastern Mediterranean Sea, *Influence of Climatic Change on the Hydrological Regime and Water Resources*, 1987, 513-523,
- Gat, J. R.: Oxygen and hydrogen isotopes in the hydrologic cycle, *Annu. Rev. Earth Planet. Sci.*, 24, 225-262, 10.1146/annurev.earth.24.1.225, 1996.
- 35



- Gat, J. R., Klein, B., Kushnir, Y., Roether, W., Wernli, H., Yam, R., and Shemesh, A.: Isotope composition of air moisture over the Mediterranean Sea: an index of the air–sea interaction pattern, *Tellus B*, 55, 953-965, 10.1034/j.1600-0889.2003.00081.x, 2003.
- Hendy, C. H.: The isotopic geochemistry of speleothems—I. The calculation of the effects of different modes of formation on the isotopic composition of speleothems and their applicability as palaeoclimatic indicators, *Geochimica et Cosmochimica Acta*, 35, 801-824, 10.1016/0016-7037(71)90127-X, 1971.
- Huang, Y., and Fairchild, I. J.: Partitioning of Sr²⁺ and Mg²⁺ into calcite under karst-analogue experimental conditions, *Geochimica et Cosmochimica Acta*, 65, 47-62, 10.1016/S0016-7037(00)00513-5, 2001.
- Karmann, I., Cruz Jr., F. W., Viana Jr., O., and Burns, S. J.: Climate influence on geochemistry parameters of waters from Santana–Pérolas cave system, Brazil, *Chemical Geology*, 244, 232-247, 10.1016/j.chemgeo.2007.06.029, 2007.
- Kim, S.-T., and O'Neil, J. R.: Equilibrium and nonequilibrium oxygen isotope effects in synthetic carbonates, *Geochimica et Cosmochimica Acta*, 61, 3461-3475, 10.1016/S0016-7037(97)00169-5, 1997.
- Klein Tank, A. M. G., Wijngaard, J. B., Können, G. P., Böhm, R., Demarée, G., Gocheva, A., Mileta, M., Pashiardis, S., Hejkrlik, L., Kern-Hansen, C., Heino, R., Bessemoulin, P., Müller-Westermeier, G., Tzanakou, M., Szalai, S., Páldóttir, T., Fitzgerald, D., Rubin, S., Capaldo, M., Maugeri, M., Leitass, A., Bukantis, A., Aberfeld, R., van Engelen, A. F. V., Forland, E., Miletus, M., Coelho, F., Mares, C., Razuvaev, V., Nieplova, E., Cegnar, T., Antonio López, J., Dahlström, B., Moberg, A., Kirchhofer, W., Ceylan, A., Pachaliuk, O., Alexander, L. V., and Petrovic, P.: Daily dataset of 20th-century surface air temperature and precipitation series for the European Climate Assessment, *International Journal of Climatology*, 22, 1441-1453, 10.1002/joc.773, 2002.
- Lachniet, M. S.: Climatic and environmental controls on speleothem oxygen-isotope values, *Quaternary Science Reviews*, 28, 412-432, 10.1016/j.quascirev.2008.10.021, 2009.
- Lloyd, J., and Taylor, J. A.: On the Temperature Dependence of Soil Respiration, *Functional Ecology*, 8, 315-323, 10.2307/2389824, 1994.
- Markowska, M., Baker, A., Andersen, M. S., Jex, C. N., Cuthbert, M. O., Rau, G. C., Graham, P. W., Rutledge, H., Mariethoz, G., Marjo, C. E., Treble, P. C., and Edwards, N.: Semi-arid zone caves: Evaporation and hydrological controls on $\delta^{18}\text{O}$ drip water composition and implications for speleothem paleoclimate reconstructions, *Quaternary Science Reviews*, 131, Part B, 285-301, 10.1016/j.quascirev.2015.10.024, 2016.
- Mattey, D. P., Fairchild, I. J., Atkinson, T. C., Latin, J.-P., Ainsworth, M., and Durell, R.: Seasonal microclimate control of calcite fabrics, stable isotopes and trace elements in modern speleothem from St Michaels Cave, Gibraltar, *Geological Society, London, Special Publications*, 336, 323-344, 10.1144/SP336.17, 2010.
- McDermott, F.: Palaeo-climate reconstruction from stable isotope variations in speleothems: a review, *Quaternary Science Reviews*, 23, 901-918, 10.1016/j.quascirev.2003.06.021, 2004.
- Pfahl, S., and Sodemann, H.: What controls deuterium excess in global precipitation?, *Clim. Past*, 10, 771-781, 10.5194/cp-10-771-2014, 2014.
- Riechelmann, D. F. C., Deininger, M., Scholz, D., Riechelmann, S., Schröder-Ritzrau, A., Spötl, C., Richter, D. K., Mangini, A., and Immenhauser, A.: Disequilibrium carbon and oxygen isotope fractionation in recent cave calcite:



- Comparison of cave precipitates and model data, *Geochimica et Cosmochimica Acta*, 103, 232-244, 10.1016/j.gca.2012.11.002, 2013.
- Sander, R.: Compilation of Henry's law constants (version 4.0) for water as solvent, *Atmos. Chem. Phys.*, 15, 4399-4981, 10.5194/acp-15-4399-2015, 2015.
- 5 Spötl, C., Fairchild, I. J., and Tooth, A. F.: Cave air control on dripwater geochemistry, Obir Caves (Austria): Implications for speleothem deposition in dynamically ventilated caves, *Geochimica et Cosmochimica Acta*, 69, 2451-2468, 2005.
- Stein, A. F., Draxler, R. R., Rolph, G. D., Stunder, B. J. B., Cohen, M. D., and Ngan, F.: NOAA's HYSPLIT atmospheric transport and dispersion modeling system, *Bull. Amer. Meteor. Soc.*, 96, 2059-2077, 10.1175/BAMS-D-14-00110.1, 2015.
- 10 Tooth, A. F., and Fairchild, I. J.: Soil and karst aquifer hydrological controls on the geochemical evolution of speleothem-forming drip waters, Crag Cave, southwest Ireland, *Journal of Hydrology*, 273, 51-68, 10.1016/S0022-1694(02)00349-9, 2003.
- Tremaine, D. M., Froelich, P. N., and Wang, Y.: Speleothem calcite farmed in situ: Modern calibration of $\delta^{18}\text{O}$ and $\delta^{13}\text{C}$ paleoclimate proxies in a continuously-monitored natural cave system, *Geochimica et Cosmochimica Acta*, 75, 4929-4950, 10.1016/j.gca.2011.06.005, 2011.
- 15 White, W.: *Geomorphology and Hydrology of Karst Terrains*, Oxford University Press, New York, 1988.
- White, W. B.: Karst hydrology: recent developments and open questions, *Engineering Geology*, 65, 85-105, 10.1016/S0013-7952(01)00116-8, 2002.

20

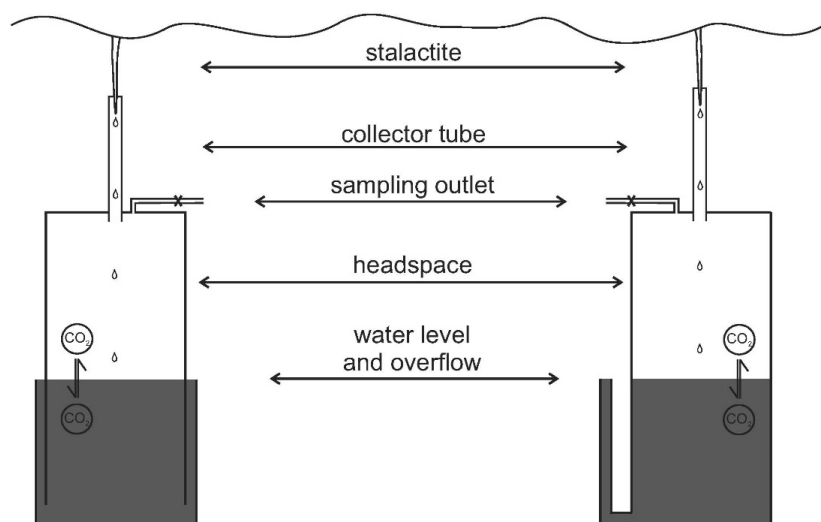


Figure 1. Schematic of the two water/air equilibrators used for the measuring of drip water CO_2 .

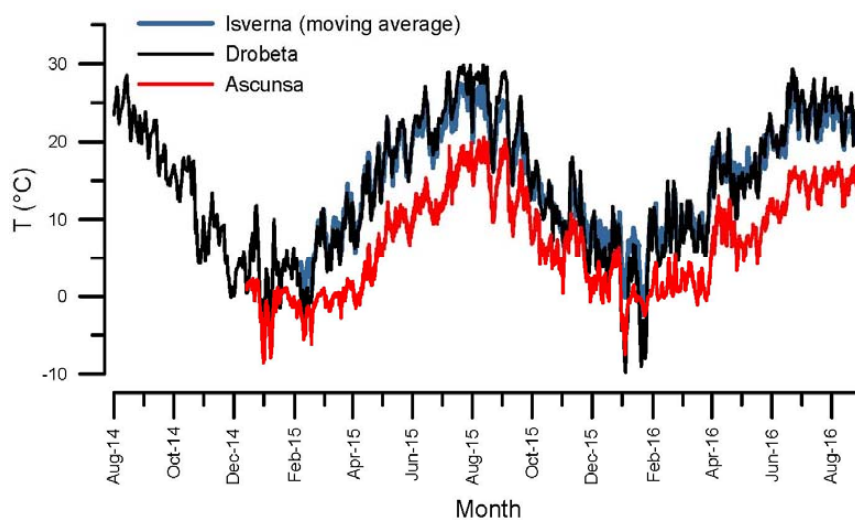
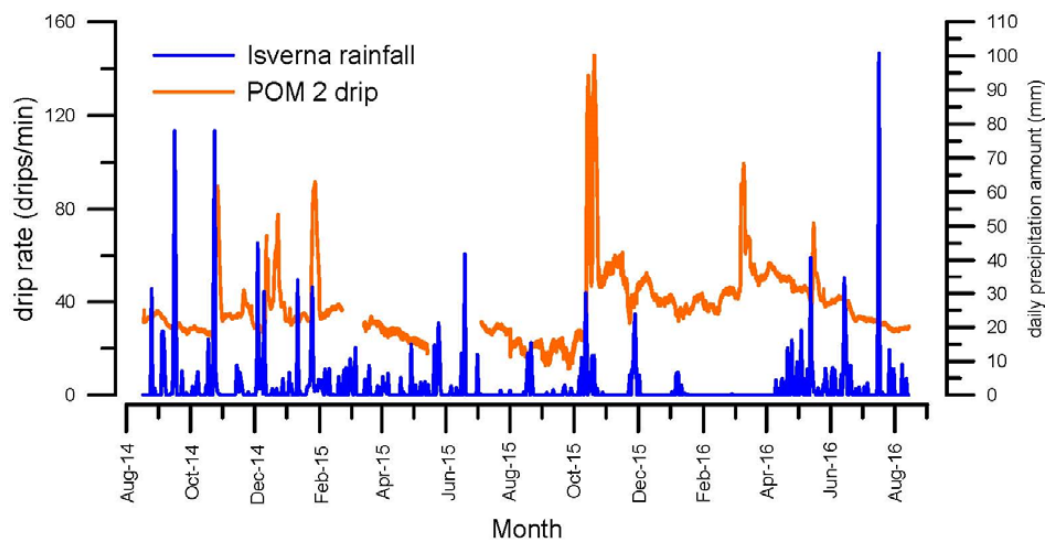


Figure 2. Temperature variability at Ascunsa Cave, Isverna and Drobeta meteorological station.



5

Figure 3. Comparison between daily precipitation amount at Isverna and POM 2drip rate.

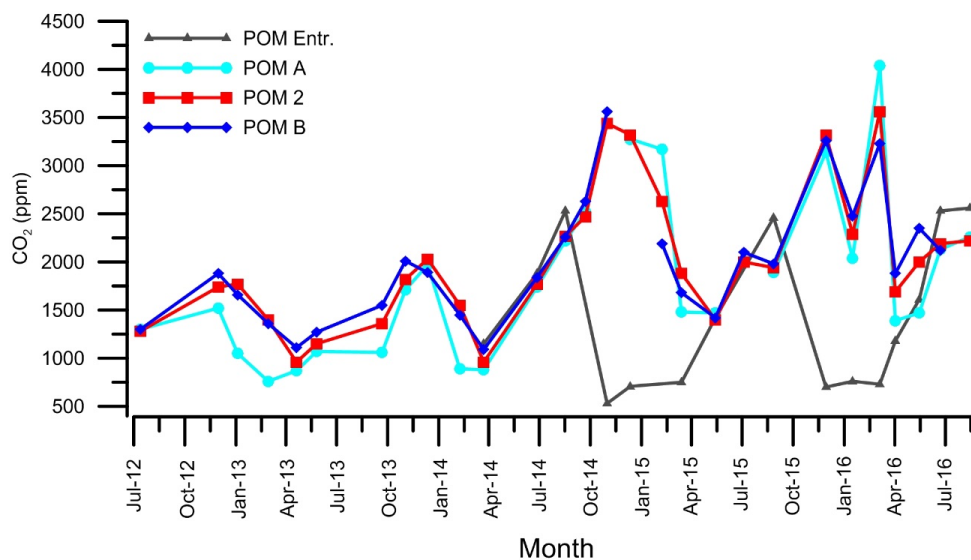


Figure 4. Cave air CO₂ concentrations at Ascunsă Cave.

5

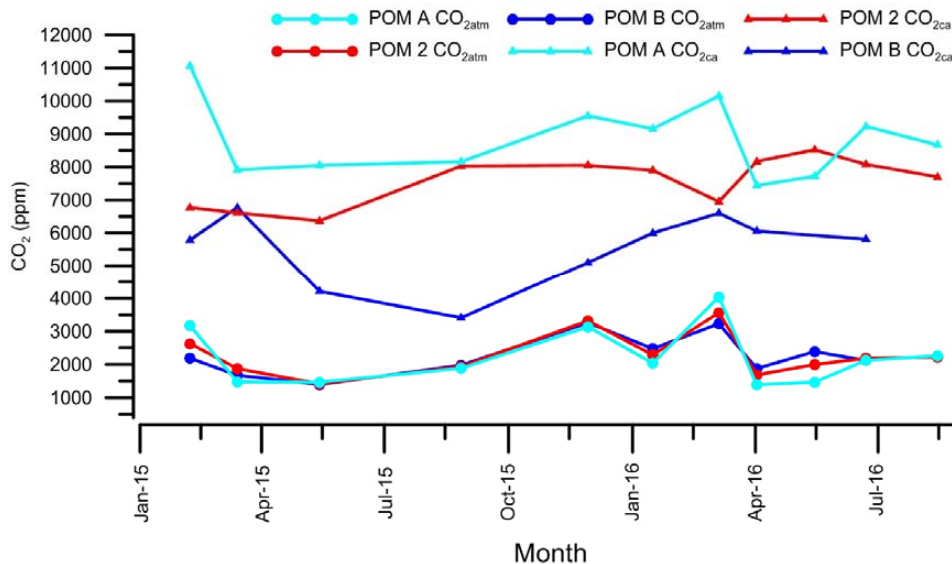


Figure 5. Comparison between CO_{2atm} and CO_{2ca}.

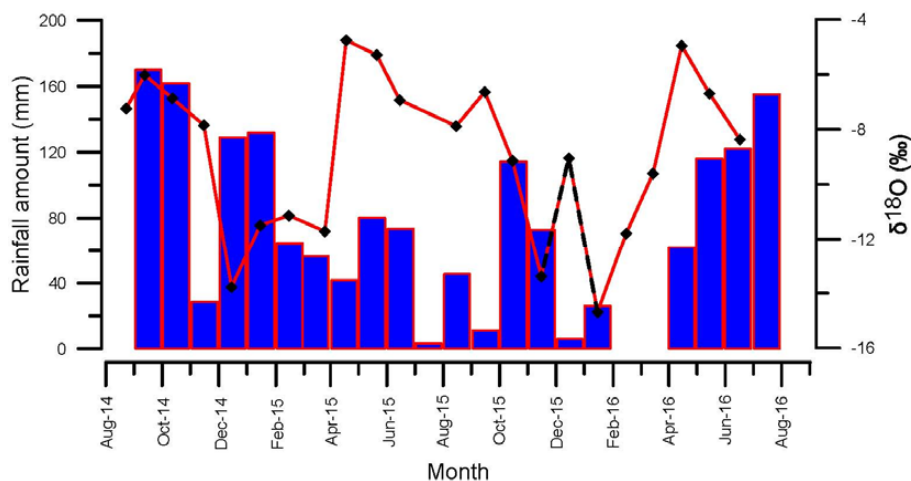
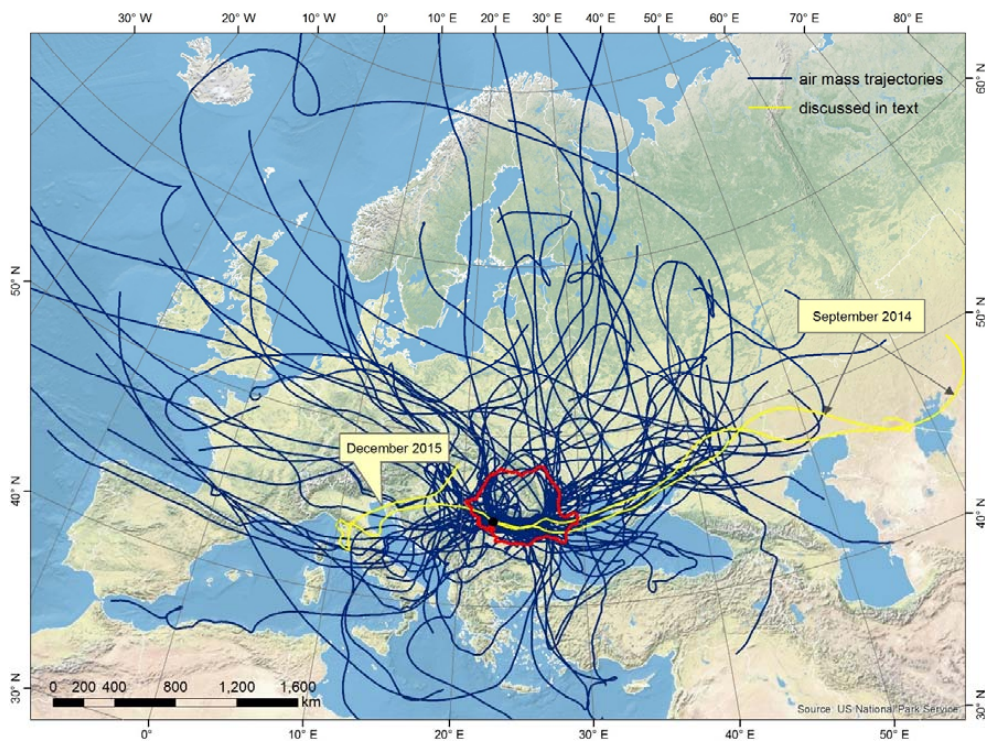


Figure 6. Monthly rainfall amounts and $\delta^{18}\text{O}$ values at Isverna.



5

Figure 7. Air mass trajectories modelled using the Hysplit 4 model.

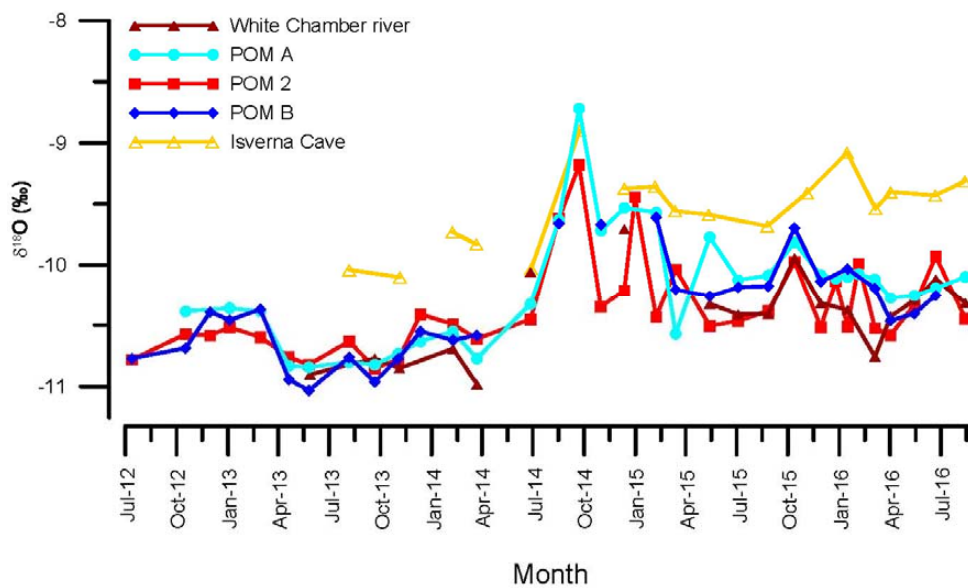


Figure 8. Drip water $\delta^{18}\text{O}$ variability at Ascunsă and Isverna caves.

5

10

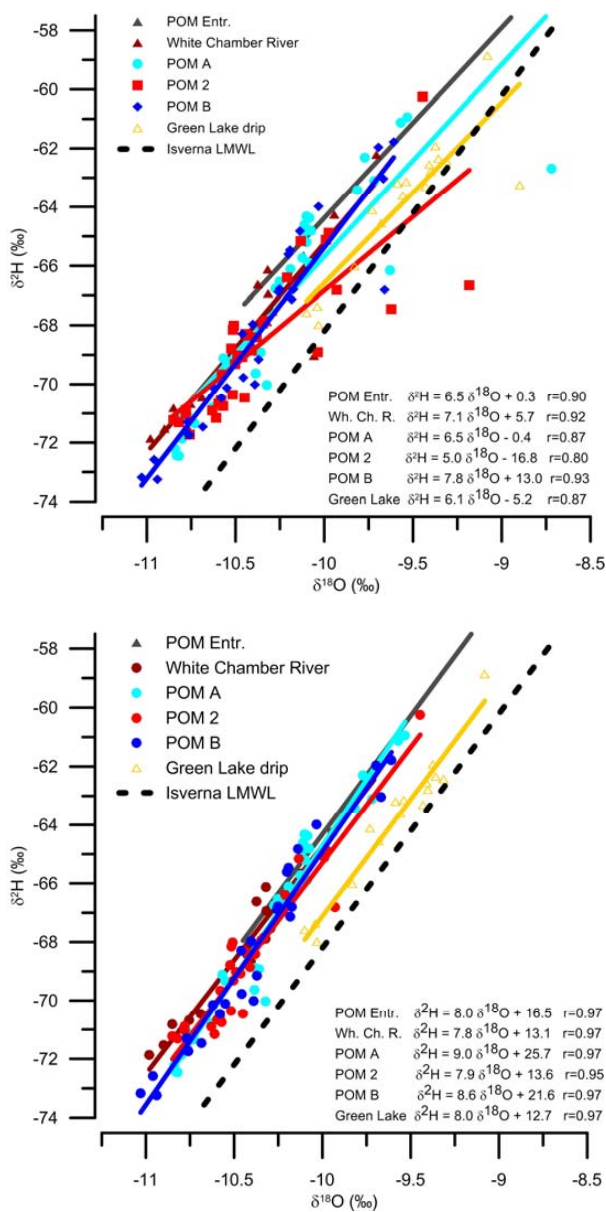


Figure 9. Water lines of drip points from Ascunsă and Isverna caves compared to the LMWL for the whole monitoring period (a) and after discarding anomalous values (b).

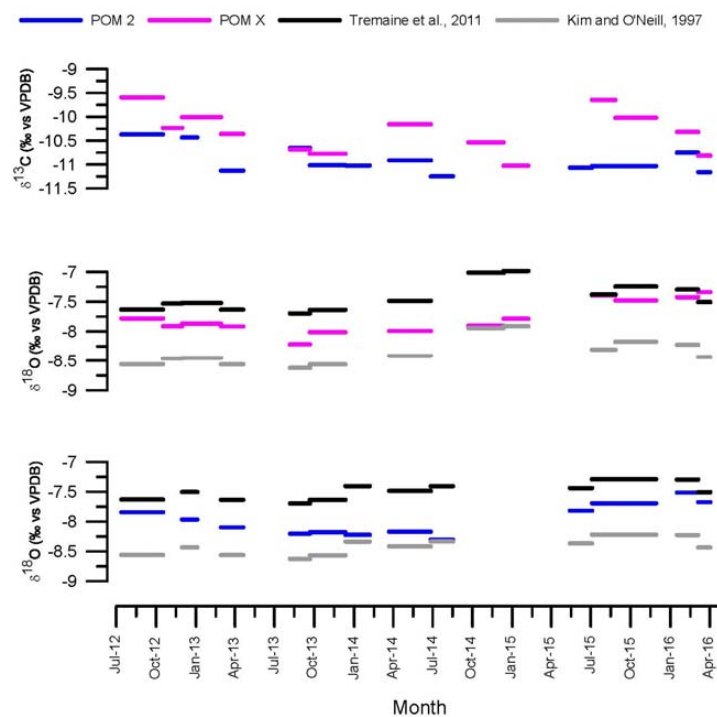


Figure 10. Stable isotope values of farmed calcite.

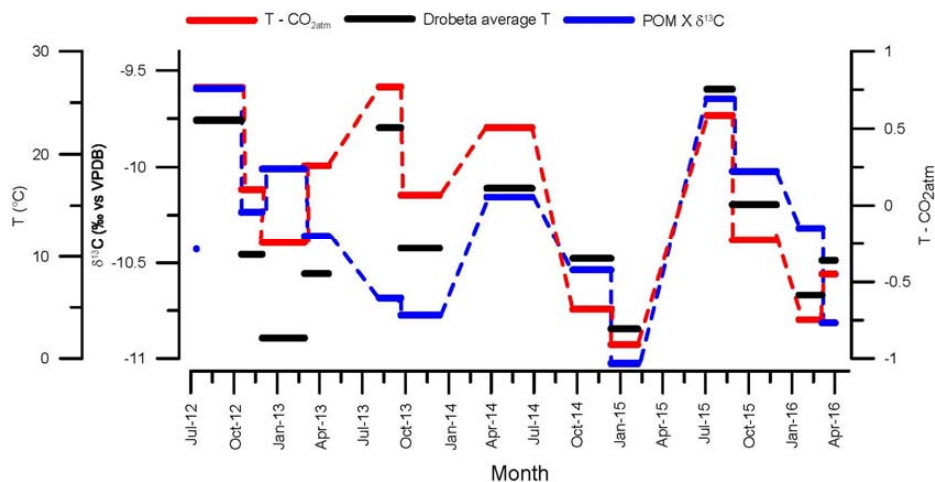


Figure 11. POM X $\delta^{13}\text{C}$ variability and its relationship with degassing gradients.